Individual Subunits of the Glutamate Transporter EAAC1 Homotrimer Function Independently of Each Other†

Christof Grewer,*,‡ Poonam Balani,§ Christian Weidenfeller,§ Thorsten Bartusel,§ Zhen Tao,‡ and Thomas Rauen*,||

University of Miami School of Medicine, 1600 NW 10th Avenue, Miami, Florida 33136, Westfälische-Wilhelms-Universität Münster, Wilhelm-Klemm-Strasse 2, D-48149 Münster, Germany, and Abteilung Biophysik, Fachbereich Biologie/Chemie, Universität Osnabrück, D-49034 Osnabrück, Germany

Received May 26, 2005; Revised Manuscript Received July 8, 2005

ABSTRACT: Glutamate transporters are thought to be assembled as trimers of identical subunits that line a central hole, possibly the permeation pathway for anions. Here, we have tested the effect of multimerization on the transporter function. To do so, we coexpressed $EAAC1_{WT}$ with the mutant transporter $EAAC1_{R446Q}$, which transports glutamine but not glutamate. Application of 50 μM glutamate or 50 μM glutamine to cells coexpressing similar numbers of both transporters resulted in anion currents of 165 and 130 pA, respectively. Application of both substrates at the same time generated an anion current of 297 pA, demonstrating that the currents catalyzed by the wild-type and mutant transporter subunits are purely additive. This result is unexpected for anion permeation through a central pore but could be explained by anion permeation through independently functioning subunits. To further test the subunit independence, we coexpressed $EAAC1_{WT}$ and $EAAC1_{H295K}$, a transporter with a 90-fold reduced glutamate affinity as compared to $EAAC1_{WT}$, and determined the glutamate concentration dependence of currents of the mixed transporter population. The data were consistent with two independent populations of transporters with apparent glutamate affinities similar to those of $EAAC1_{H295K}$ and $EAAC1_{WT}$, respectively. Finally, we coexpressed $EAAC1_{WT}$ with the pH-independent mutant transporter $EAAC1_{E373Q}$, showing two independent populations of transporters, one being pH-dependent and the other being pH-independent. In conclusion, we propose that EAAC1 assembles as trimers of identical subunits but that the individual subunits in the trimer function independently of each other.

Plasma-membrane glutamate transporters actively remove glutamate from the synaptic cleft after excitatory neurotransmission is complete. Uptake into the cells surrounding the synapse against a glutamate concentration gradient is achieved by these transporters by coupling transmembrane glutamate movement to the cotransport of three sodium ions and one proton and the countertransport of one potassium ion (*1*, *2*). In addition to the movement of ions across the membrane being directly coupled to glutamate transport, glutamate transporters also catalyze uncoupled transmembrane flux of anions (*3*). This anion conductance is thought to be an integral property of the transporters and is not mediated by indirect coupling of transport to a secondary anion channel (*3*−*5*).

The mammalian glutamate transporters belong to a large family of membrane transport proteins that comprise also neutral amino acid transporters, such as the alanine serine cysteine transporters [ASCTs[1] (*6*, *7*)] and dicarboxylate transporters (*8*, *9*). A large number of biochemical data from both mammalian (*10*, *11*) and bacterial glutamate transporters (*12*, *13*), as well as recent crystallographic evidence from a glutamate transporter from a thermophilic bacterium [GltP (*14*)] showed that the polypeptide chain spans the membrane 8 times and that two reentrant loops dip into the membrane, one from the extracellular side and one from the intracellular side. The crystal structure of GltP also showed that three monomers of the transporter coassemble in a trimeric protein with an unusual, bowl-shaped structure (*14*). However, the crystal structure of GltP gives no insight into

† This work was supported by the National Institutes of Health Grant R01-NS0493 to C.G. and by the Deutsche Forschungsgemeinschaft Grants GR 1393/2-2,3 to C.G. and RA 753/1-1,2 to T.R. Z.T. is grateful for a postdoctoral fellowship by the American Heart Association (0525485B).

* To whom correspondence should be addressed: Department of Physiology and Biophysics, University of Miami School of Medicine, 1600 NW 10th Avenue, Miami, FL 33136. Telephone: (305) 243-1021. Fax: (305) 243-5931. E-mail: cgrewer@med.miami.edu (C.G.); Abteilung Biophysik, Fachbereich Biologie/Chemie, Universität Osnabrück, D-49034 Osnabrück, Germany. Telephone: 0541-6689709. E-mail: rauen@biologie.uni-osnabrueck.de (T.R.).

‡ University of Miami School of Medicine.

§ Westfälische-Wilhelms-Universität Münster.

|| Universität Osnabrück.

[1] Abbreviations: EAAC1, excitatory amino acid carrier 1; EAAT, excitatory amino acid transporter; ASCT, alanine serine cysteine transporter; GltP, glutamate transporter homologue from *Pyrococcus horikoshii*; PBS, phosphate-buffered saline; HEPES, 4-(2-hydroxyethyl)-1-piperazineethanesulfonic acid; TEA, tetraethylammonium; EGTA, ethylene glycol-bis-(β-aminoethyl ether)-*N*,*N*,*N*′,*N*′-tetracetic acid; EDTA, ethylenediaminetetraacetic acid; HEK, human embryonic kidney; DTT, dithiothreitol; SDS, sodium dodecyl sulfate; PAGE, polyacrylamide gel electrophoresis; BMDB, 1,4-bismaleimidyl-2,3-dihydroxybutane; TG, transglutaminase; BS^3, bis(sulfosuccinimidyl)suberate; Co-IP, co-immunoprecipitation; TBOA, DL-*threo*-β-benzyloxyaspartate; GFP, green fluorescent protein; YFP, yellow fluorescent protein; Bzl-Ser, benzylserine; MW, molecular weight.

10.1021/bi050987n CCC: $30.25
Published on Web 08/10/2005

the functional importance of the trimeric assembly of the transporter.

The mammalian members of the glutamate transporter protein family appear to be also assembled as trimers. In 1996, Haugeto et al. reported the first evidence for multimeric assembly of natively expressed brain glutamate transporters (*15*). Although freeze-fracture electron microscopy data from *Xenopus* oocytes expressing the excitatory amino acid transporter 3 (EAAT3) seemed to indicate pentameric assembly (*16*), it was later shown in two reports that EAAT2 (*14*, *17*) forms a trimeric structure. However, independent of the number of co-assembled subunits, the effects of multimerization on the mechanism of glutamate uptake and on the functional properties of the anion conductance of the transporters are unknown. A number of models have been proposed to account for the experimental data (*5*, *16*). In one model, both glutamate transport and anion conductance are mediated by a central pore in the oligomeric subunit assembly (*16*). In this model, only one glutamate molecule could be transported at a time by each oligomer. Although this model seems unlikely in the light of the crystal structure of GltP, which appears to have binding sites for glutamate on each subunit of the trimer (*14*), there is no functional data available that would contradict this model. In a second model, glutamate transport is mediated by the individual subunits, whereas anion permeation occurs through a central pore (*5*). A third model includes both anion permeation and glutamate transport through the individual subunits of the oligomer (*5*). The last two models would allow for cooperativity of glutamate uptake, i.e., conformational coupling of and cross-talk between transporter subunits. At present, there is no experimental data available to differentiate between these functional models.

Here, we asked the question whether the individual subunits in the trimeric assembly function independently of one another or if there is cross-talk between the subunits. We addressed this question by coexpressing wild-type EAAC1 with transporters that have been mutated in specific regions to affect their functional properties. Trimeric co-assembly of EAAC1 and the mutant transporters was confirmed by Western blotting. In one set of experiments, the wild-type transporter was coexpressed with $EAAC1_{R446Q}$, which converts the EAAC1 from a glutamate transporter to a neutral amino acid transporter, similar to the R446C exchange published by the Kanner group (*18*). Coexpression of mutant and wild-type subunits resulted in carriers that transported glutamate and alanine independently of each other. Furthermore, specific inhibition of one subunit did not affect substrate transport by the other subunit. When our experiments were taken together with data from the coexpressing wild-type and $EAAC1_{H295K}$ and $EAAC1_{E373Q}$ mutant transporters, they suggest that the EAAC1 forms trimers but that the individual subunits of the trimers work independently of each other. Furthermore, our data suggest that the anion conductance of glutamate transporters is mediated by the individual subunits, rather than a central pore.

EXPERIMENTAL PROCEDURES

Molecular Biology and Transient Expression. Wild-type EAAC1 cloned from rat retina was subcloned into pBK-CMV (Stratagene) as described previously (*19*) and was subjected to site-directed mutagenesis according to the QuikChange protocol (Stratagene, La Jolla, CA) as described by the supplier. Cys-less EAAC1 was produced by the same procedure by sequentially mutating the five cysteine residues in $EAAC1_{WT}$ (C9, C158, C218, C255, and C342) to serine. The primers for mutagenesis were obtained from the DNA core lab, Department of Biochemistry at the University of Miami School of Medicine. The complete coding sequences of mutated EAAC1 clones were subsequently sequenced. Wild-type and mutant EAAC1 constructs (named pCMV-$EAAC1_{WT}$ or pCMV-$EAAC1_{mutantform}$) were used for transient transfection of subconfluent human embryonic kidney cell (HEK293, ATCC number CGL 1573 or HEK293T/17, ATCC number CRL 11268) cultures using the calcium phosphate-mediated transfection method (*20*) as described previously (*19*, *21*). For coexpression experiments, cDNAs of the mutant and wild-type receptors were used for transfection in a 1:1 ratio, unless stated otherwise. Electrophysiological recordings were performed between days 1 and 3 post-transfection.

Membrane Vesicle Preparation and Cross-Linking. Glutamate transporter-expressing HEK293 cells were homogenized on ice in 10 mM 4-(2-hydroxyethyl)-1-piperazineethanesulfonic acid (HEPES)-NaOH at pH 7.4 containing 100 mM NaCl, 1 mM Na_4-EDTA, and Protease-Inhibitor Complete (Roche Applied Science, Mannheim, Germany) in a dilution according to the instructions of the manufacturer and centrifuged for 10 min at 400*g* to remove nuclei, cell debris, and undisrupted cells (P1 fraction). The supernatant was centrifuged for 30 min at 30000*g* at 4 °C. The resulting pellet (P2 fraction/membrane vesicles) was processed according to the respective cross-linking protocols (Supporting Information). Cross-linking products were analyzed by sodium dodecyl sulfate−polyacrylamide gel electrophoresis (SDS−PAGE) and Western blotting. Controls were processed under identical conditions prior to and after the experiment, however, without adding enzymatic or chemical cross-linkers (see lanes 1 and 6 in A−F of Figure 3 and Figure 10 in the Supporting Information, respectively). The experimental procedures for chemical and enzymatic cross-linking can be found in the Supporting Information.

SDS−PAGE and Western-Blot Analysis. Cross-linking products were separated and analyzed by SDS−PAGE using a 6% separating gel (0.5 mm thick) and Western-blot analysis. Immunoblots were prepared with affinity-purified antibodies directed against EAAC1 (BioTrend Chemikalien GmbH, Köln, Germany) in a dilution of 1:1000 as described previously (*22*). The antibody reaction was detected by chemiluminescence using Hyperfilm-ECL (Amersham ECL-Detection kit; Amersham Biosciences U.K. Limited, Little Chalfont, U.K.). To determine the apparent molecular weight (MW) of the cross-linking products, the Pre-stained Protein Marker, Broad Range (6.5−175 kDa) (New England Biolabs, Beverly, MA) was used in parallel with "HiMark" High Molecular Protein Standard (40−500 kDa) (Invitrogen GmbH, Karlsruhe, Germany) to determine molecular weights higher than 175 kDa. MW marker proteins on immunoblots were stained with Protogold (Plano GmbH, Wetzlar, Germany). The MW of each cross-linking product was determined using the gel documentation software Total Lab (Nonlinear Dynamics, Newcastle upon Tyne, U.K.).

Co-immunoprecipitation. Transfected HEK293 cells were washed 2 times with phosphate-buffered saline (PBS; 137 mM NaCl, 2.7 mM KCl, 10 mM Na_2HPO_4, and 2 mM KH_2PO_4 at pH 7.4). Cells were collected after adding cell lysis buffer (20 mM Tris at pH 7.5, 150 mM NaCl, 1 mM EDTA, 1% Triton X-100, and protease inhibitor cocktail 2, Sigma) by mechanical trituration. Cell membranes were further broken down by freezing and thawing 3 times and then passing through a 26-gauge needle 10 times. The resulting suspension was centrifuged at 1000*g* for 10 min to remove debris. The concentration of the supernatant (cell lysate) was adjusted to 1 μg/μL. Protein A agarose beads (Upstate) were added to 500 μL of cell lysate and incubated for 1 h with gentle rocking at 4 °C to preclear the cell lysate. After centrifugation and transfer of the supernatant to another tube, anti-GFP antibody (BioVision) was added and the solution was incubated with gentle rocking overnight at 4 °C. Protein A agarose beads were added and incubated with gentle rocking for 2 h at 4 °C. The beads were washed 3 times with 500 μL of cell lysis buffer. Protein was eluted from the beads with 2× Laemmli buffer, and the sample was heated to 65 °C for 10 min. The sample was loaded onto a 10% SDS−PAGE gel and analyzed by Western blotting, and protein bands were detected with the ECL reagent.

Electrophysiology and Rapid Solution Exchange. Glutamate-induced EAAC1 currents were recorded with an Adams and List EPC7 amplifier under voltage-clamp conditions in the whole-cell current-recording configuration (*23*). The typical resistance of the recording electrode was 2−3 MΩ; the series resistance was 5−8 MΩ. Because the glutamate-induced currents were small (typically <500 pA), series resistance (R_S) compensation had a negligible effect on the magnitude of the observed currents (<4% error). Therefore, R_S was not compensated. The extracellular solution contained 140 mM NaCl, 2 mM $CaCl_2$, 2 mM $MgCl_2$, and 30 mM HEPES. Two different pipet solutions were used depending on whether mainly the noncoupled anion current (with thiocyanate) or the coupled transport current (with chloride) was investigated (*19*, *24*). These solutions contained 130 mM KSCN or KCl, 2 mM $MgCl_2$, 10 mM tetraethylammonium chloride (TEACl), 10 mM ethylene glycol-bis-(β-aminoethyl ether)-*N*,*N*,*N*′,*N*′-tetracetic acid (EGTA), and 10 mM HEPES (pH 7.4/KOH). Thiocyanate was used because it enhances glutamate transporter-associated currents and allows the detection of the EAAC1 anion-conducting mode (*19*, *25*).

For the electrophysiological investigation of the Na^+/glutamate homoexchange mode (*24*), the pipet solution contained 140 mM NaCl/NaSCN, 2 mM $MgCl_2$, 10 mM TEACl, 10 mM EGTA, 10 mM glutamate, and 10 mM HEPES (pH 7.4/NaOH). In this transport mode, the same concentrations of Na^+ are used on both sides of the membrane, and concentrations of glutamate are used on the intra- and extracellular side, which saturate their respective binding sites. The affinity of EAAC1 for cytoplasmic glutamate is 280 μM (*26*). Therefore, we used 10 mM cytoplasmic glutamate to ensure saturation of the intracellular binding site. In contrast, the affinity for extracellular glutamate is about 6 μM (*19*), and 100−200 μM extracellular glutamate is sufficient for saturation of this binding site. When permeating anions, such as SCN^-, are present, establishment of homoexchange conditions leads to the permanent activation of an anion current (*24*, *27*, *28*). This permanent anion current was used in this work as a tool to study the behavior of mutant transporters in the homoexchange mode.

The currents were low-pass-filtered at 1−10 kHz (Krohn-Hite 3200) and digitized with a digitizer board (Axon, Digidata 1200) at a sampling rate of 10−50 kHz, which was controlled by software (Axon PClamp). All of the experiments were performed at room temperature.

Rapid solution exchange was performed as described previously (*19*). Briefly, substrates were applied to the EAAC1-expressing cell by means of a quartz tube (opening diameter of 350 μm) positioned at a distance of ∼0.5 mm to the cell. The linear flow rate of the solutions emerging from the opening of the tube was ∼5−10 cm/s, resulting in typical rise times of the whole-cell current of 30−50 ms (10−90%).

Data Analysis. Nonlinear regression fits of experimental data were performed with Origin (Microcal software, Northampton, MA) or Clampfit (pClamp8 software, Axon Instruments, Foster City, CA). Dose−response data were described with a Michaelis−Menten-type relationship. To describe the properties of mixed populations of wild-type and mutant transporters, we used a sum of two Michaelis−Menten-type equations.

RESULTS

Our experiments were designed to test the functional consequences of the trimeric structure of the glutamate transporter. For this purpose, we used coexpression of wild-type EAAC1 with mutant transporters. The first mutant EAAC1 that we coexpressed with the wild-type transporter was $EAAC1_{R446Q}$ (see Figure 1A for an illustration of the localization of the mutated residues within the EAAC1 structure). It had been previously shown that neutralization of the conserved arginine residue in position 446 converts EAAC1 from a transporter specific for acidic amino acids to one that is specific for neutral amino acids, such as alanine (*18*). Our objective was to generate heterotrimers that contain subunits activated by either glutamate or alanine but not by both substrates.

Functional Characterization of $EAAC1_{R446Q}$. We first tested the specificity of $EAAC1_{R446Q}$ expressed in HEK293 cells for neutral amino acids. When 500 μM alanine was applied to $EAAC1_{R446Q}$ in the homoexchange mode (140 mM NaSCN and 10 mM alanine internal, see Figure 1B for a graphical illustration of the transport modes used), it generated a large inwardly directed anion current (left panel of Figure 1C), caused by the outward movement of SCN^-. In contrast, application of 500 μM glutamate to the same cell did not result in any detectable current (middle panel of Figure 1C). Similar results were obtained for concentrations of glutamate up to 1 mM (Figure 1D). The typical glutamate concentration used in the coexpression experiments was 50 μM. Thus, these results demonstrated that glutamate does not activate the anion current in $EAAC1_{R446Q}$ at the typical concentrations used.

The alanine-induced current was dependent on the alanine concentration (Figure 1D), saturating with an apparent K_m of 20.1 ± 1.0 μM ($n = 3$). On average, the alanine-induced anion current at saturating alanine concentrations was −398

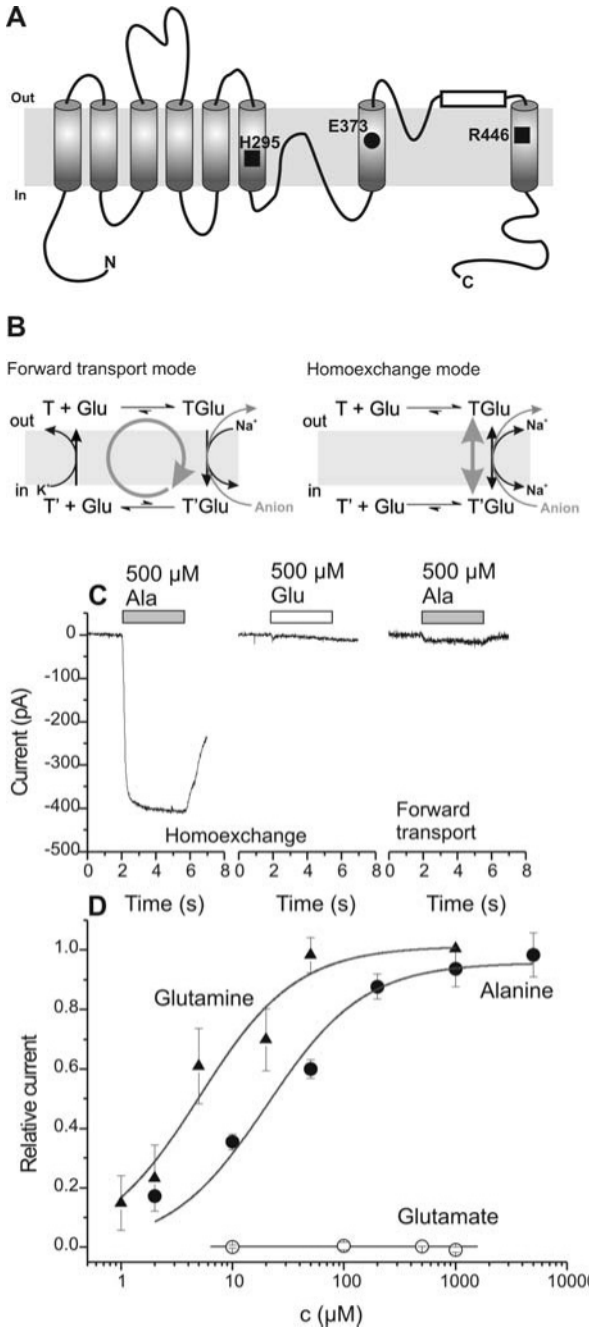

FIGURE 1: (A) Topology of EAAC1 and the location of the mutated amino acid residues. (B) Graphical illustration of the transport modes studied. (C) Glutamate does not activate $EAAC1_{R446Q}$. Typical inward currents are shown in response to the application of 500 μM alanine to a cell expressing $EAAC1_{R446Q}$ (left panel). The middle panel shows the response of the same cell to an application of 500 μM glutamate (140 mM NaSCN, 10 mM alanine, and 10 mM glutamate in the recording pipet solution). Application of 500 μM alanine in the presence of intracellular KSCN (forward transport conditions) evokes very little current (right panel). (D) Dose−response relationships for alanine and glutamate under recording conditions as in C. The solid lines represent best fits according to a Michaelis−Menten-like relationship. All recordings were performed at 0 mV transmembrane potential.

$\pm$ 155 pA (from 12 cells). This compared well to the -475 ± 120 pA (from 20 cells) obtained for glutamate activation of $EAAC1_{WT}$ anion current under homoexchange conditions, showing that the R446Q amino acid exchange did not result in a dramatically changed expression level of the mutant as compared to the wild-type transporter. In addition to alanine,

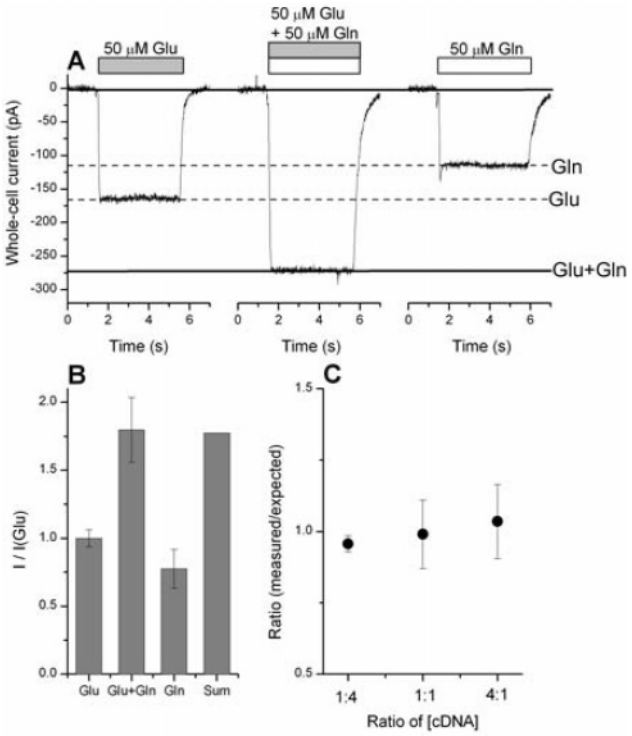

FIGURE 2: Anion current responses to glutamate and glutamine of WT/R446Q mixed transporter populations are purely additive. (A) 50 μM glutamate (left trace), 50 μM glutamine (right trace), and 50 μM glutamate and 50 μM glutamine (middle trace) were applied to a cell expressing both $EAAC1_{WT}$ and $EAAC1_{R446Q}$ after transfection with a 1:1 mixture of the respective cDNAs. The line marked Glu represents the current level evoked by glutamate application, and the line marked Gln represents the current evoked by glutamine application. The baseline was adjusted to 0. Currents were recorded in the exchange mode (140 mM NaSCN, 5 mM glutamine, and 5 mM glutamate in the recording pipet solution). (B) Statistical analysis of the data shown in A ($n = 5$). (C) Ratio of experimentally determined and expected currents as a function of the ratio of the transfected cDNA concentration for purely statistical coassembly of the trimer. The expected currents were calculated from a binomial distribution with probabilities of finding one of the two subunits in the trimeric assembly of 0.2 (ratio 1:4), 0.5 (ratio 1:1), and 0.8 (ratio 4:1), respectively.

we also tested glutamine as a substrate for $EAAC1_{R446Q}$. As shown in Figure 1D, glutamine generated maximum anion currents indistinguishable from the alanine-induced currents but activated the transporter with a 4 times higher apparent affinity of 5.1 ± 1.0 μM ($n = 3$). Finally, we tested whether alanine and glutamine are substrates for $EAAC1_{WT}$. At the concentration range used for the coexpression experiments (up to 500 μM), no activation of anion current was observed for either of these two neutral amino acids, indicating that they were not recognized as substrates by $EAAC1_{WT}$.

Properties of Mixed $EAAC1_{WT}$−$EAAC1_{R446Q}$. Next, we characterized the functional properties of a mixed population of wild-type and R446Q mutant transporters. Initially, these experiments were performed in the homoexchange mode because $EAAC1_{R446Q}$ does not catalyze steady-state forward transport (right panel of Figure 1C). Application of 50 μM glutamate to HEK293 cells expressing a mixed population of these transporters resulted in generation of inwardly directed anion current (left panel of Figure 2A). A slightly smaller anion current ($I_{Gln}/I_{Glu} = 0.78 \pm 0.13$, $n = 5$) was induced by 50 μM glutamine (right panel of Figure 2A). When both substrates were applied at the same time, the

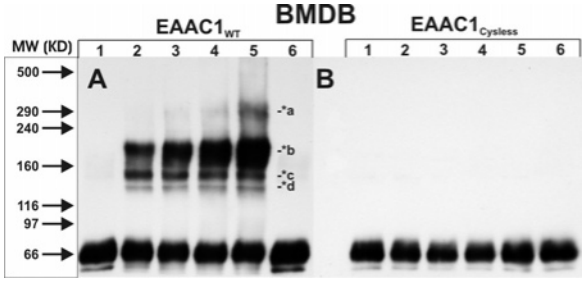

FIGURE 3: Thiol-specific cross-linking of the heterologously expressed wild-type EAAC1 and the cysteine-less mutant of EAAC1. Hypotonically washed membranes derived from $EAAC1_{WT}$ (A) or $EAAC1_{cysless}$ (B) expressing HEK293 cells were incubated with 25 μM BMDB (lanes 2−5 in A and B, respectively). The cross-linking reaction was stopped after incubation times of 10, 30, 60, and 120 min. Controls (non-crosslinked membranes before and after the experimental procedure; starting material, lanes 1; postexperimental, lanes 6) and cross-linking products (10 μg of total membrane protein/lane) were separated by 6% SDS−PAGE and were immunoblotted with EAAC1-specific antibodies. Molecular mass markers (left panels, MW) are indicated in kilodaltons. The data shown are representative of at least three independent experiments.

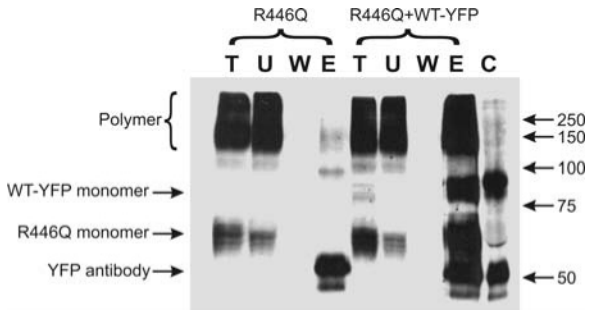

FIGURE 4: Co-immunoprecipitation results. $EAAC1_{WT}$ and $EAAC1_{R446Q}$ were co-immunoprecipitated with a $EAAC1_{WT}$−YFP fusion protein by using an anti-GFP antibody. Total (T), unbound (U), washed (W), and eluted (E) samples were loaded on 10% SDS−PAGE. The corresponding amount of anti-GFP was also loaded as a control (C). Protein was transferred to a nylon membrane and detected by anti-EAAC1 antibody and ECL reagent. The left four lanes were samples from cells transfected with $EAAC1_{R446Q}$ alone; the right four lanes were samples from cells transfected with $EAAC1_{R446Q}$ plus $EAAC1_{WT}$−YFP.

anion current was 1.80 ± 0.21 times the current in the presence of only glutamate (middle panel of Figure 2A), suggesting that the currents induced by the two substrates are purely additive, pointing to independent operation of the subunits of the trimer. The statistical analysis of the results from 5 cells is shown in Figure 2B.

To test for statistical coassembly of $EAAC1_{WT}$ and $EAAC1_{R446Q}$, we expressed the two proteins in varying amounts by altering the cDNA ratio used for the transfection from 1:4 to 4:1. As shown in Figure 2C, the ratio of the currents induced by glutamate and alanine was in agreement with that expected for pure statistical coassembly of the wild-type and mutant transporters.

Although it has been previously shown that EAAT2 forms homotrimers (*14*, *17*), the subunit stoichiometry of EAAC1 has so far not been determined by using biochemical methods. Therefore, we used Western blotting to test whether EAAC1 also assembled as a trimer. We used a cross-linking approach based on three different cross-linking reagents, two chemical [thiol specific (BMDB) and amino specific (BS^3)] and one enzymatic cross-linking approach (transglutaminase reaction). Cross-linking with BMDB resulted in the formation of two prominent bands after Western blotting (Figure 3A), corresponding to the monomer (69 kDa) and trimer [200 kDa (*b in Figure 3A)]. In addition, some lower intensity bands were observed that indicated the formation of dimers and a higher molecular weight species, possibly a tetramer. Multimer formation was not observed when a cysteine-less variant of EAAC1 was treated with BMDB (Figure 3B). A detailed description of the cross-linking data, including cross-linking with BS^3 and transglutaminase, can be found in the Supporting Information. Together, the cross-linking data suggest that EAAC1 forms homotrimers.

To directly test whether $EAAC1_{R446Q}$ can co-assemble with wild-type EAAC1, we performed co-immunoprecipitation (co-IP) experiments. Wild-type transporter and $EAAC1_{R446Q}$ were coexpressed with an $EAAC1_{WT}$−YFP fusion protein. Anti-GFP antibody was used to perform the co-IP. Proteins were separated by 10% SDS−PAGE and analyzed by Western blot with anti-EAAC1 as the primary antibody. As shown in Figure 4, the $EAAC1_{R446Q}$ protein was co-immunoprecipitated from cells that coexpress $EAAC1_{R446Q}$ and $EAAC1_{WT}$−YFP. No $EAAC1_{R446Q}$ protein was co-immunoprecipitated from cells that expressed $EAAC1_{R446Q}$ alone, which excluded the possibility that anti-GFP antibody can interact with $EAAC1_{R446Q}$. As a control, co-immunoprecipitation of wild-type transporter and $EAAC1_{WT}$−YFP was also performed with similar results (data not shown). These results clearly show that $EAAC1_{R446Q}$ can co-assemble with wild-type EAAC1.

So far, we have characterized the glutamate and alanine translocation properties of $EAAC1_{WT}$−$EAAC1_{R446Q}$ by locking the transporters in the homoexchange mode. Because the translocation of the K^+-bound transporter form is impaired in $EAAC1_{R446Q}$, we next measured steady-state transport currents in the mixed population of transporters, to test whether cooperativity of the subunits is required for the relocation reaction. As shown in Figure 5A (left panel), application of 50 μM glutamate to the transporters in the forward transport mode resulted in the activation of large anion currents (−290 ± 70 pA, $n = 4$, KSCN intracellular solution), even in the total absence of alanine. This result suggested that occupation of the alanine-binding site of $EAAC1_{R446Q}$ was not required for forward glutamate transport in the wild-type transporter. As expected, application of 200 μM alanine in the forward transport mode to the same cells generated only 13% of the glutamate-induced inward anion currents (−39 ± 11 pA, $n = 4$, middle panel of Figure 5A). Application of both substrates at the same time resulted in an anion current that was purely additive, as shown in the right panel of Figure 5A.

The magnitude of the anion current carried by SCN^- outflow is a good measure for the forward transport activity of wild-type and mutant glutamate transporters, because it is believed that anion conductance is associated with few specific states within the transport cycle, such as the Na^+, H^+, and glutamate-bound states (see for example refs *19*, *24*, *28*, and *29*). Furthermore, it was shown that the anion current is absent when steady-state transport is inhibited in the wild-type transporter or by specific mutants such as E373Q (*21*) and R446Q (this work). However, to directly test the effect of subunit interaction on glutamate transport,

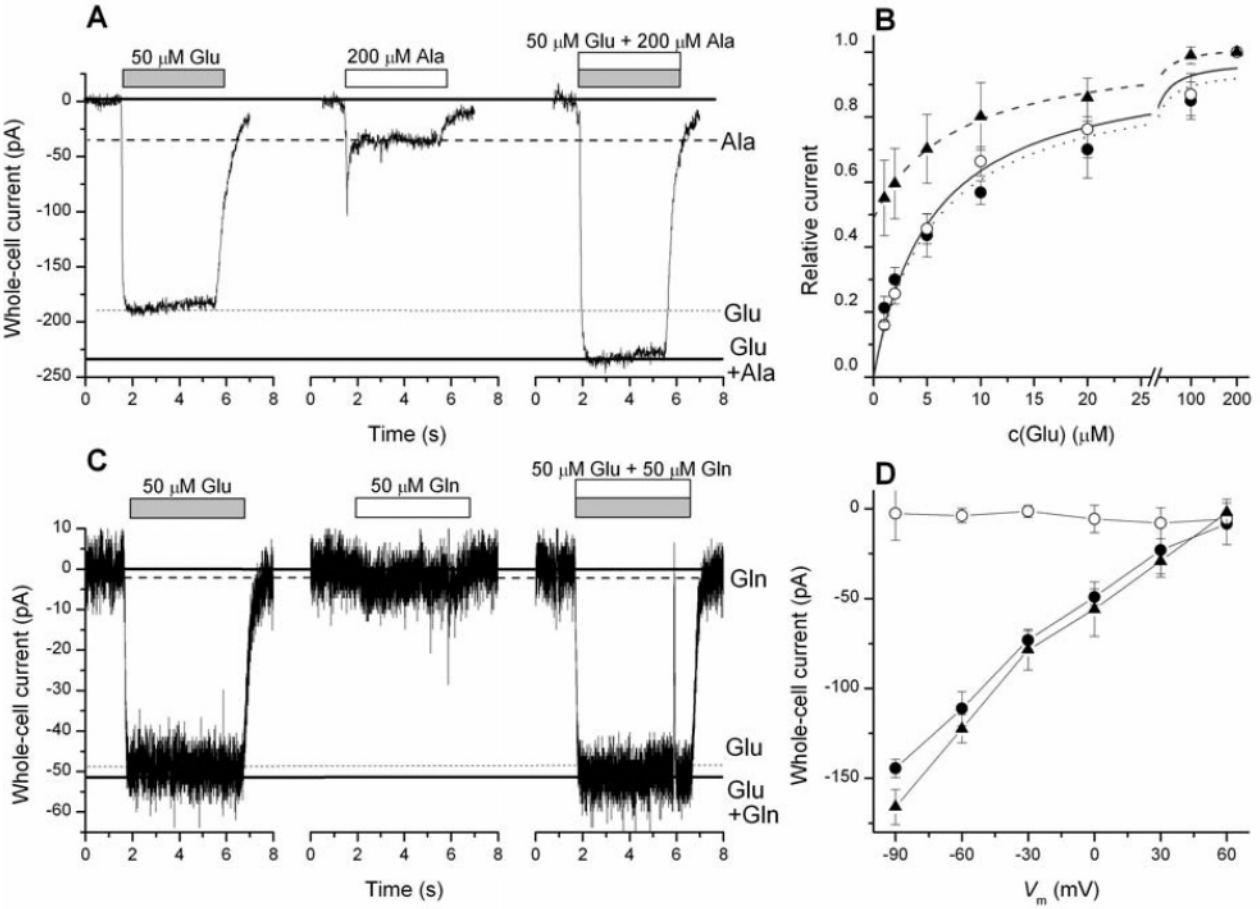

FIGURE 5: Forward transport of $EAAC1_{WT}$ is not inhibited in the presence of equal amounts of $EAAC1_{R446Q}$. (A) 50 μM glutamate (left panel), 200 μM alanine (middle panel), and 50 μM glutamate and 200 μM alanine (right panel) were applied to a cell expressing both $EAAC1_{WT}$ and $EAAC1_{R446Q}$ after transfection with a 1:1 mixture of the respective cDNAs. The line marked *Glu* represents the current level evoked by glutamate application; *Ala* represents the current evoked by alanine application; and *Glu* + *Ala* represents the current level in the presence of both substrates. The baseline was adjusted to 0. Anion currents were recorded in the forward transport mode in the presence of permeating anions (140 mM KSCN in the recording pipet solution). (B) Glutamate dose−response curves recorded in the absence (○) and the presence (● and ▲) of 500 μM extracellular alanine. The data shown as ○ and ● were recorded in the presence of intracellular KSCN (forward transport mode). (▲) Experiments performed in the homoexchange mode (140 mM NaSCN, 5 mM glutamate, and 5 mM alanine internal) in the presence of 500 μM extracellular alanine. The data were obtained at 0 mV transmembrane potential. The dashed line represents a fit to a Michaelis−Menten-like equation with an additional *y*-offset parameter. The solid and dotted lines are fits according to a Michaelis−Menten equation. (C) Transport currents induced in $EAAC1_{WT}$ and $EAAC1_{R446Q}$ coexpressing cells by application of 50 μM glutamate (left panel), 50 μM glutamine (middle panel), and 50 μM glutamate and 50 μM glutamine (right panel). The baseline was adjusted to 0. Currents were recorded in the forward transport mode in the absence of permeating anions (140 mM KCl in the recording pipet solution). (D) Voltage dependence of transport currents under conditions similar as in C. Transport currents were recorded in the presence of 50 μM glutamate (●), 50 μM glutamine (○), and 50 μM glutamate and 50 μM glutamine (▲).

we measured transport currents in the absence of a driving force for anions across the membrane (symmetrical Cl^- concentrations on both sides of the membrane, 0 mV, Figure 5C), to confirm the results obtained from the anion currents in the forward transport mode. As expected, 50 μM glutamate elicited inward transport currents in mixed $EAAC1_{WT}$−$EAAC1_{R446Q}$ transporters (−48 ± 2 pA, $n = 4$, KCl intracellular solution), even in the absence of alanine or glutamine (left panel of Figure 5C). In contrast, application of 50 μM glutamine did not induce any measurable currents (−1 ± 1 pA, $n = 4$, middle panel of Figure 5C). The same result was found throughout the tested range of transmembrane potentials from −90 to +60 mV (Figure 5D). The absence of glutamine-induced currents was not due to the absence of $EAAC1_{R446Q}$ transporters, because application of glutamine to the same batch of cells in the presence of 140 mM extracellular SCN^- resulted in the activation of outwardly directed anion currents (+220 ± 34 pA, $n = 4$, 140 mM NaCl and 10 mM alanine-containing intracellular solution).

To further test for cross-talk between the individual subunits, we determined whether the substrate affinity of one subunit depended on the occupancy of a neighboring subunit in the trimer. In trimers that contained only the wild-type transporter, the K_m for glutamate in the homoexchange mode was 13 μM. For trimers that contained both $EAAC1_{WT}$ and $EAAC1_{R446Q}$ transporters, the K_m for glutamate was 8.9 ± 1.0 μM ($n = 3$) in the absence of alanine. In the presence of 500 μM alanine, the K_m for glutamate did not change within experimental error (8.0 ± 1.1 μM, $n = 3$, Figure 5B). The same experiments were repeated in the forward transport mode. In this mode, the substrate-binding sites of $EAAC1_{R446Q}$ should be mainly exposed to the intracellular side in the presence of alanine. We found a K_m for glutamate of 5.4 ± 0.6 μM ($n = 3$, Figure 5B) in the absence of alanine and 5.6 ± 1.1 μM ($n = 3$, Figure 5B) in the presence of alanine.

Together, these results suggest that the substrate affinity of one subunit in the trimer is independent of the state of the neighboring subunits.

Finally, we tested specific competitive inhibitors of either the wild-type transporter or $EAAC1_{R446Q}$ for their effects in the mixed trimer. The glutamate transporter inhibitor DL-*threo*-β-benzyloxyaspartate (TBOA) is a potent inhibitor of EAAC1 with a K_i in the submicromolar range (*19*, *30*), but it did not block alanine-induced currents in $EAAC1_{R446Q}$ at concentrations up to 200 μM. When 100 μM TBOA was applied to trimers containing both the wild-type transporter and $EAAC1_{R446Q}$, an outward current was induced ($+44 \pm 4$ pA, $n = 3$, left panel of Figure 6A). This outward current was caused by inhibition of the sustained leak anion conductance of EAAC1 in the presence of intracellular SCN^- (*19*, *31*). However, TBOA did not inhibit the inward anion current generated by 500 μM alanine (left panel of Figure 6A). In addition, we used benzylserine, which is a competitive inhibitor of the neutral amino acid transporter ASCT2 (*32*). Benzylserine (1 mM) did not induce any currents in EAAC1, but it generated outward current in $EAAC1_{R446Q}$, because of the inhibition of the sustained anion leak (determined by the voltage dependence of the benzylserine-induced current, data not shown), which is conserved in this mutant transporter. The apparent affinity of $EAAC1_{R446Q}$ for benzylserine was determined to 160 ± 10 μM ($n = 4$, data not shown). In the mixed $EAAC1_{WT}-EAAC1_{R446Q}$ trimer, application of 1 mM benzylserine also resulted in outward current ($+49 \pm 5$ pA, $n = 3$, left panel of Figure 6B). Similar to TBOA, however, benzylserine did not significantly inhibit glutamate-elicited inward current (left panel of Figure 6B). When both inhibitors where applied at the same time, an outward current of 84 ± 9 pA ($n = 3$) was observed, which is 91% of the current expected if both inhibitors inhibited their respective subunits independently. The results are statistically summarized in Figure 6C. Together, these results indicated that inhibition of one subunit in the trimer did not affect the function of the neighboring subunits.

Properties of Mixed $EAAC1_{WT}-EAAC1_{H295K}$ Oligomers. Thus far, the data obtained from the coexpression experiments with the wild-type and R446Q transporters did not strictly exclude the possibility that glutamate and the cotransported cations are transported through a single pore in the middle of the trimeric subunit assembly. To test this possibility, we coexpressed the wild-type transporter with $EAAC1_{H295K}$. We had shown previously that $EAAC1_{H295K}$ has a dramatically reduced affinity for glutamate (*33*). Therefore, we expected that coexpression of $EAAC1_{WT}$ and $EAAC1_{H295K}$ would produce transporters with an affinity intermediate of the wild-type and the mutant transporter, if both mutant and wild-type subunits would line a central permeation pathway for glutamate. In contrast, the experimental dose−response curve for glutamate shown in Figure 7A could not be described by a Michaelis−Menten-like relationship with intermediate glutamate affinity (dotted line in Figure 7A) but was rather consistent with two independent populations of transporters with K_m values for glutamate of 7.4 ± 0.9 and 730 ± 80 μM ($n = 4$), respectively. These K_m values fit very well with the K_m of the pure wild-type and H295K transporters of 13 and 600 ± 60 μM ($n = 5$), respectively, as illustrated by the dashed lines in Figure 7A. The contribution of the $EAAC1_{H295K}$ current to the total current of the mixed population was 43 ± 4%, in agreement with previous findings, showing that $EAAC1_{H295K}$ catalyzes

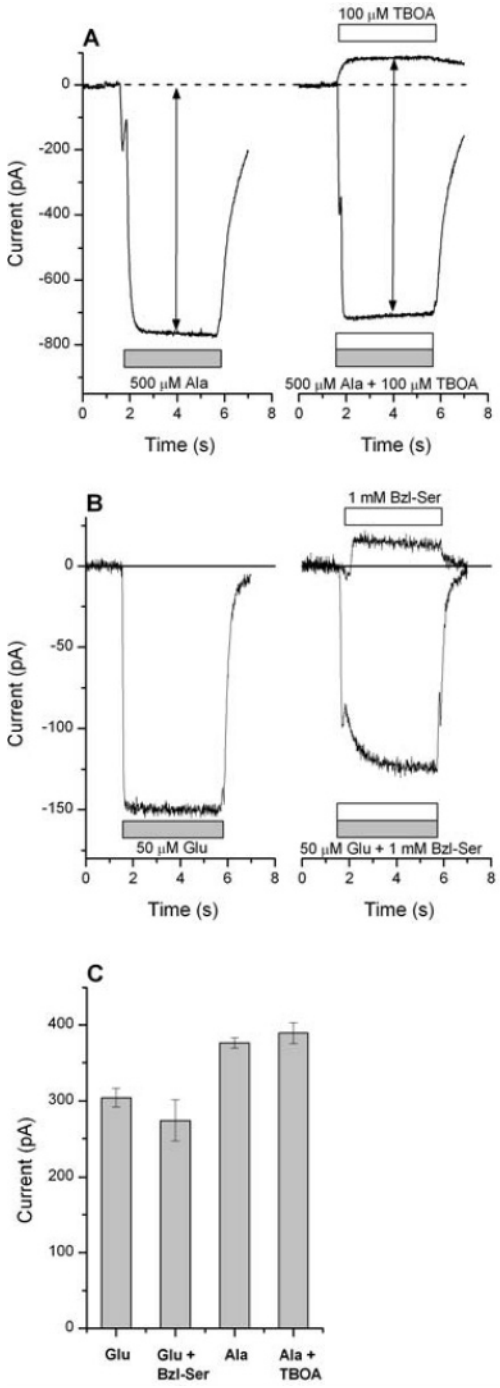

FIGURE 6: Inhibition of individual transporter subunits by competitive inhibitors does not exert a dominant negative effect. (A) (Left panel) Anion current evoked by the application of 500 μM alanine to a mixed population of $EAAC1_{WT}$ and $EAAC1_{R446Q}$. (Right panel) Application of 100 μM TBOA, a competitive inhibitor of $EAAC1_{WT}$, to the same cell evokes an outward current (upper trace). The lower trace shows the response to both 500 μM alanine and 100 μM TBOA. All currents were recorded in the homoexchange mode. (B) (Left panel) Anion current evoked by the application of 50 μM glutamate to a mixed population of $EAAC1_{WT}$ and $EAAC1_{R446Q}$. (Right panel) Application of 1 mM Bzl-Ser, a competitive inhibitor of $EAAC1_{R446Q}$, to the same cell evokes an outward current (upper trace). The lower trace shows the response to both 50 μM glutamate and 1 mM Bzl-Ser. The arrow represents the total glutamate-induced current response in the absence and presence of Bzl-Ser. All currents were recorded at 0 mV voltage with a SCN^--containing pipet solution. (C) Statistical analysis of the data shown in A and B ($n = 4$).

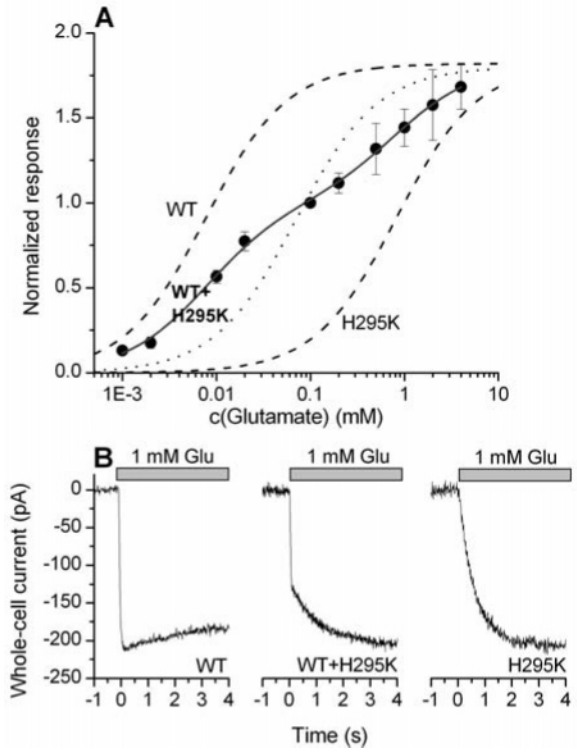

FIGURE 7: (A) Dose−response relationship of a mixed population of $EAAC1_{WT}$ and $EAAC1_{H295K}$ transporters activated by glutamate. The dashed lines represent the dose−response relationships of pure $EAAC1_{WT}$ and $EAAC1_{H295K}$ transporters. The solid line represents the best fit of a sum of two Michaelis−Menten-like relationships to the data, assuming an independent population of WT and mutant transporters. The dotted line represents a Michaelis−Menten-like relationship calculated with a K_m intermediate between the wild-type and mutant EAAC1. The cDNAs for the mutant and wild-type transporters were mixed in a 1:1 ratio. The recording pipet contained 140 mM NaSCN and 10 mM glutamate ($V_m = 0$ mV). (B) Current responses to 1 mM glutamate application to HEK293 cells expressing wild-type EAAC1 (left panel), $EAAC1_{H295K}$ (right panel), and a mixed population of wild-type transporter and $EAAC1_{H295K}$ under the same conditions as in A.

less anion current than wild-type EAAC1 (*33*).

In addition to having a dramatically different K_m for glutamate, $EAAC1_{H295K}$ has the effect of slowing the activation of the glutamate-induced anion current by about a factor of 100 (*33*), as shown in Figure 7B. Whereas application of 1 mM glutamate to $EAAC1_{WT}$ resulted in a single-exponential anion current activation with a time constant of 45 ± 5 ms (left panel of Figure 7B), which reflects the time resolution of the rapid solution exchange system, activation of the anion current in $EAAC1_{H295K}$ occurred with a time constant of 790 ± 5 ms ($n = 4$, right panel of Figure 7B). In contrast to the single-exponential rising behavior of the pure transporters, anion currents of the mixed population of wild-type and H295K transporters were activated with a double-exponential time course (middle panel of Figure 7B). The time constants for the two phases of the current rise were 33 ± 3 and 1090 ± 40 ms, respectively. These results suggested that the kinetic properties of the mixed wild-type and H295K mutant transporters can be described by a simple sum of the kinetic properties of the individual transport proteins.

Properties of Mixed $EAAC1_{WT}$−$EAAC1_{E373Q}$. The glutamate residue E373 is conserved in the mammalian glutamate transporter family (*34*) but not in ASC transporters (*6*, *21*).

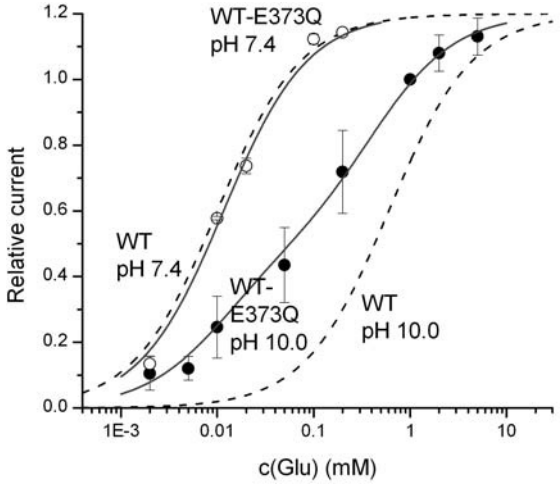

FIGURE 8: Dose−response relationship of a mixed population of $EAAC1_{WT}$ and $EAAC1_{E373Q}$ transporters activated by glutamate at pH 7.4 (○) and 10.0 (●). The dashed lines represent the dose−response relationships of $EAAC1_{WT}$ at pH values of 7.4 and 10.0. The solid lines represent the best fit of a sum of two Michaelis−Menten-like relationships to the data at pH 7.4 and 10.0, assuming an independent population of WT and mutant transporters (ratio of cDNA concentrations of 1:1). The data were collected in the presence of 140 mM Na^+ and 10 mM glutamate in the cytosol (homoexchange conditions).

We had previously proposed that E373 is involved in proton cotransport by EAAC1, because the E373Q mutation abolishes the intrinsic pH dependence of glutamate transport (*21*). Here, we coexpressed $EAAC1_{WT}$ with $EAAC1_{E373Q}$ and determined the functional properties of the mixed transporters as a function of the extracellular pH. At pH 7.3, $EAAC1_{WT}$ and $EAAC1_{E373Q}$ have very similar apparent affinities for glutamate (*19*), 13 and 10 μM, respectively. Consistently, the dose−response relationship of the mixed transporter population, shown in Figure 8 (○), was well-described by a Michaelis−Menten-like relationship with an apparent K_m of 12.6 ± 1.2 μM ($n = 3$). In contrast, the dose−response relationship was more complex at an extracellular pH of 10.0 (● in Figure 8). Assuming an additive response of $EAAC1_{WT}$ and $EAAC1_{E373Q}$ to glutamate, the dose−response curve could be described by a sum of two Michaelis−Menten-like curves, one yielding an apparent K_m of 11.3 ± 0.3 μM and the other component yielding a K_m of 420 ± 71 μM. These results are consistent with the existence of two independent transporter populations, one being the wild-type transporter with a shift of the K_m to 610 μM at pH 10.0 [right dotted line in Figure 8 (*26*)] and the other being $EAAC1_{E373Q}$ with its virtually pH-independent K_m that remains at 17 μM at pH 10 (*21*).

DISCUSSION

In this study, we report that the individual subunits of the glutamate transporter subtype EAAC1 homotrimer function independently of each other. To reach this conclusion, we used three different mutant transporters, which have dramatically different substrate specificity and kinetic properties than those of the wild type, and coexpressed them with the wild-type transporters. In one of the mutant transporters, the substrate specificity is changed from recognition of acidic amino acids to recognition of neutral amino acids, by an arginine 446 to glutamine exchange. This mutation allowed

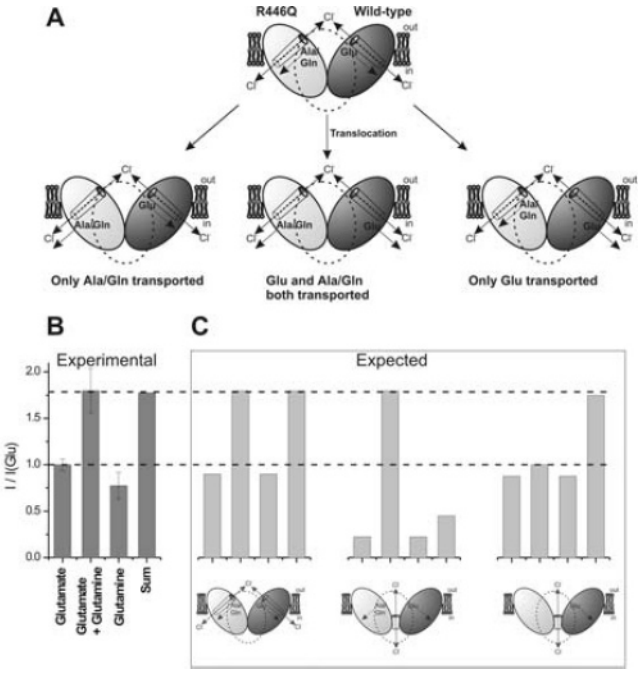

FIGURE 9: (A) Proposed model for the independent action of subunits of $EAAC1_{WT}$ (dark gray, transports Glu) and $EAAC1_{R446Q}$ (light gray, transports either Ala or Gln) in the heterotrimeric unit. The model shows a side view of the transporter according to the crystal structure of Yernool et al. (*12*). The third subunit is represented by the dashed line. The cylinder represents the anion permeation pathway. (B and C) Comparison of experimental currents (B) and expected currents (C) induced upon coapplication of glutamate and glutamine to the mixed population of transporters according to three different models. In the left model, both subunits work independently and anion permeation is through pathways on individual subunits (see also A). In the middle model, anion permeation is through a central pathway and needs binding of both ligands to be activated. In the right model, anion permeation is through a central pathway and needs binding of only one of the two ligands to be activated. The expected currents were calculated based on a binomial distribution with a probability of finding each of the two subunits in a trimeric assembly of 0.5 (1:1 coexpression of the wild-type and mutant transporters).

us to assemble EAAC1 trimers, which contain subunits that can either bind glutamate or alanine. Thus, we were able to determine that the occupancy of one subunit binding site within the trimer has no functional effects on substrate transport by a neighboring subunit. Our data are consistent with the lack of cooperativity found for glutamate transport by EAAC1. Numerous functional studies showed that the Hill coefficient for the glutamate concentration dependence of transport is close to one (*19*, *36*−*39*), suggesting that only one glutamate molecule needs to be bound to the transporter at a time to induce transport. Although it can be difficult to draw conclusions about cooperativity based only on Hill coefficients, our data provide the simplest explanation for the Hill coefficient of 1; namely, that it does not matter whether the substrate-binding site of a neighboring subunit is occupied or not, glutamate always binds with the same affinity and is transported with the same rate. Thus, it seems that there is no cross-talk between the individual transporter subunits. The model that we propose for independent functioning of the glutamate transporter subunits is graphically illustrated in Figure 9A.

Our conclusions are based on the assumption that the mutant and wild-type subunits coassemble to a functional trimer. Although our functional data would also be consistent with a model in which mutant and wild-type transporters only form homotrimers but not heterotrimers, we can reject this possibility for several reasons. First, we were able to directly show that one of the mutant transporters, $EAAC1_{R446Q}$, coassembles with wild-type EAAC1 by co-immunoprecipitating $EAAC1_{R446Q}$ with an $EAAC1_{WT}$−YFP fusion protein. Second, we investigated transporters with three different mutations in different transmembrane segments of EAAC1. It appears unlikely that all three mutations would have the same inhibitory effect on subunit assembly. Third, none of the mutations investigated is close to the subunit interface of the glutamate transporter multimer. This multimerization interface is mainly composed of transmembrane segments 2, 4, and 5 (*14*). The mutations generated here are localized in transmembrane helices 6, 7, and 8. Transmembrane helix 6, which contains the H296K mutation, is localized on the outer, membrane-facing side of the transporter unit, which is on the opposite side of the subunit interface (*14*).

Our data allow us to exclude possible mechanistic models that were previously discussed for glutamate transport and catalysis of the anion conductance by the multimeric assembly of subunits (*5*). In one model, both glutamate transport and anion conductance are through the same pathway, which is a central pore in the middle of the subunits. This model would predict mixed properties of transporter assemblies between mutant and wild-type transporters, which are between the properties of the pure transporters. The data presented here exclude this model. Instead of observing transporters with mixed properties, we always observe independent populations of transporters that have either the properties of the mutant or the wild-type transporter but not intermediate properties. In a second model, anion conductance is through a central pore and can be gated by cooperative binding of the substrate to all three subunits (middle panel of Figure 9C). This second model is analogous to typical mechanistic models for ligand-gated ion channels. This model is clearly not consistent with our data (Figure 9B), because we would expect that in the $EAAC1_{WT}$−$EAAC1_{R446Q}$ mixed transporter anion current would be only generated in the presence of both glutamate and glutamine, which is experimentally not observed (middle panel of Figure 9C). Third, a model would be possible in which anion conductance is through a central pore that can be activated by binding the substrate to only one of the three subunits (right panel of Figure 9C). This model can be excluded, because it would be expected that in the $EAAC1_{WT}$−$EAAC1_{R446Q}$ mixed transporter the presence of one substrate alone would be sufficient to elicit the maximum anion-conductance activation. Again, this is experimentally not found (right panel of Figure 9C).

Some predictions of experimental data of these models are summarized in Figure 9C. It is clear that the model shown in Figure 9A predicts the experimental data well (left panel of parts B and C of Figure 9), whereas the other models do not result in a satisfactory prediction. The model includes anion permeation through the individual subunits and not through a central pore. This interpretation is consistent with a previous report showing that the anion conductance is tightly associated with Na^+ binding to the transporter (*24*, *40*). Although the location of the Na^+-binding sites cannot be directly deduced from the recently published crystal

structure of GltP (*14*), it seems unlikely that sodium ion binding occurs near the center of the trimeric subunit assembly. The central vestibule is composed of mainly hydrophobic amino acid residues and is too narrow for ion permeation (*14*). Thus, it is likely that the anion-permeation pathway is associated within the center of each individual subunit, which constitutes probably also the permeation pathway for the substrate and cotransported Na^+ ions. This conclusion is in agreement with data published in ref *4*, showing that some amino acid residues in transmembrane segments 2 affect the anion-permeation properties upon mutation. These amino acid residues do not compose a central anion-permeation pathway (*14*).

The model of individual functioning of the subunits of the trimer proposed here has also implications for our understanding of the molecular machinery of the glutamate transporter. The crystal structure of GltP shows a large, water-filled bowl in the center of the three subunits (*12*). Although this bowl might be filled in the mammalian transporters with the protein mass from the extracellular loop between transmembrane helices 3 and 4, it would be tempting to speculate on an alternating access mechanism in which the bowl and therefore the glutamate-binding site would be exposed either to the extracellular or to the intracellular side of the membrane in a cooperative, large-scale conformational reorganization of the whole protein complex. However, the data presented here exclude such a model, because it would require cooperativity between the individual subunits. On the basis of the data, we favor a model that requires only small conformational changes of the individual subunits upon glutamate binding, which are not transmitted to the neighboring subunits. These conformational changes might take place only in the C-terminal part of the transporter and are shielded from the subunit interface by transmembrane domains 2, 4, and 5. Thus, it is possible that helices 2−6 form a structural scaffold that protects the functionally important C-terminal part from interaction with the lipid bilayer and the neighboring subunits.

While this manuscript was in preparation, a study had been published that also suggests independent functioning of glutamate transporter subunits (*41*). This study reached the same conclusions by using a very different approach from ours, namely, chemical modification of mutant transporters at cysteine residues.

SUPPORTING INFORMATION AVAILABLE

Detailed description of the chemical and enzymatic cross-linking experiments and the Western blotting data for BS^3 and TG cross-linking. This material is available free of charge via the Internet at http://pubs.acs.org.

REFERENCES

1. Kanner, B. I., and Bendahan, A. (1982) Binding order of substrates to the sodium and potassium ion coupled L-glutamic acid transporter from rat brain, *Biochemistry 21*, 6327−6330.
2. Zerangue, N., and Kavanaugh, M. P. (1996) Flux coupling in a neuronal glutamate transporter, *Nature 383*, 634−637.
3. Wadiche, J. I., Amara, S. G., and Kavanaugh, M. P. (1995) Ion fluxes associated with excitatory amino acid transport, *Neuron 15*, 721−728.
4. Ryan, R. M., Mitrovic, A. D., and Vandenberg, R. J. (2004) The chloride permeation pathway of a glutamate transporter and its proximity to the glutamate translocation pathway, *J. Biol. Chem. 24*, 24.
5. Slotboom, D. J., Konings, W. N., and Lolkema, J. S. (2001) Glutamate transporters combine transporter- and channel-like features, *Trends Biochem. Sci. 26*, 534−539.
6. Broer, A., Brookes, N., Ganapathy, V., Dimmer, K. S., Wagner, C. A., Lang, F., and Broer, S. (1999) The astroglial ASCT2 amino acid transporter as a mediator of glutamine efflux, *J. Neurochem. 73*, 2184−2194.
7. Zerangue, N., and Kavanaugh, M. P. (1996) ASCT-1 is a neutral amino acid exchanger with chloride channel activity, *J. Biol. Chem. 271*, 27991−27994.
8. Finan, T. M., Oresnik, I., and Bottacin, A. (1988) Mutants of *Rhizobium meliloti* defective in succinate metabolism, *J. Bacteriol. 170*, 3396−3403.
9. Finan, T. M., Wood, J. M., and Jordan, D. C. (1981) Succinate transport in *Rhizobium leguminosarum*, *J. Bacteriol. 148*, 193−202.
10. Brocke, L., Bendahan, A., Grunewald, M., and Kanner, B. I. (2002) Proximity of two oppositely oriented reentrant loops in the glutamate transporter GLT-1 identified by paired cysteine mutagenesis, *J. Biol. Chem. 277*, 3985−3992.
11. Grunewald, M., Bendahan, A., and Kanner, B. I. (1998) Biotinylation of single cysteine mutants of the glutamate transporter GLT-1 from rat brain reveals its unusual topology, *Neuron 21*, 623−632.
12. Slotboom, D. J., Lolkema, J. S., and Konings, W. N. (1996) Membrane topology of the C-terminal half of the neuronal, glial, and bacterial glutamate transporter family, *J. Biol. Chem. 271*, 31317−31321.
13. Slotboom, D. J., Sobczak, I., Konings, W. N., and Lolkema, J. S. (1999) A conserved serine-rich stretch in the glutamate transporter family forms a substrate-sensitive reentrant loop, *Proc. Natl. Acad. Sci. U.S.A. 96*, 14282−14287.
14. Yernool, D., Boudker, O., Jin, Y., and Gouaux, E. (2004) Structure of a glutamate transporter homologue from *Pyrococcus horikoshii*, *Nature 431*, 811−818.
15. Haugeto, O., Ullensvang, K., Levy, L. M., Chaudhry, F. A., Honore, T., Nielsen, M., Lehre, K. P., and Danbolt, N. C. (1996) Brain glutamate transporter proteins form homomultimers, *J. Biol. Chem. 271*, 27715−27722.
16. Eskandari, S., Kreman, M., Kavanaugh, M. P., Wright, E. M., and Zampighi, G. A. (2000) Pentameric assembly of a neuronal glutamate transporter, *Proc. Natl. Acad. Sci. U.S.A. 97*, 8641−8646.
17. Gendreau, S., Voswinkel, S., Torres-Salazar, D., Lang, N., Heidtmann, H., Detro-Dassen, S., Schmalzing, G., Hidalgo, P., and Fahlke, C. (2004) A trimeric quaternary structure is conserved in bacterial and human glutamate transporters, *J. Biol. Chem. 279*, 39505−39512.
18. Bendahan, A., Armon, A., Madani, N., Kavanaugh, M. P., and Kanner, B. I. (2000) Arginine 447 plays a pivotal role in substrate interactions in a neuronal glutamate transporter, *J. Biol. Chem. 275*, 37436−37442.
19. Grewer, C., Watzke, N., Wiessner, M., and Rauen, T. (2000) Glutamate translocation of the neuronal glutamate transporter EAAC1 occurs within milliseconds, *Proc. Natl. Acad. Sci. U.S.A. 97*, 9706−9711.
20. Chen, C., and Okayama, H. (1987) High-efficiency transformation of mammalian cells by plasmid DNA, *Mol. Cell. Biol. 7*, 2745−2752.
21. Grewer, C., Watzke, N., Rauen, T., and Bicho, A. (2003) Is the glutamate residue Glu-373 the proton acceptor of the excitatory amino acid carrier 1? *J. Biol. Chem. 278*, 2585−2592.
22. Rauen, T., Rothstein, J. D., and Wassle, H. (1996) Differential expression of three glutamate transporter subtypes in the rat retina, *Cell Tissue Res. 286*, 325−336.
23. Hamill, O. P., Marty, A., Neher, E., Sakmann, B., and Sigworth, F. J. (1981) Improved patch-clamp techniques for high-resolution current recording from cells and cell-free membrane patches, *Pflugers Arch. Eur. J. Physiol. 391*, 85−100.
24. Watzke, N., Bamberg, E., and Grewer, C. (2001) Early intermediates in the transport cycle of the neuronal excitatory amino acid carrier EAAC1, *J. Gen. Physiol. 117*, 547−562.
25. Bergles, D. E., and Jahr, C. E. (1997) Synaptic activation of glutamate transporters in hippocampal astrocytes, *Neuron 19*, 1297−1308.

26. Watzke, N., Rauen, T., Bamberg, E., and Grewer, C. (2000) On the mechanism of proton transport by the neuronal excitatory amino acid carrier 1, *J. Gen. Physiol. 116*, 609−622.
27. Bergles, D. E., Tzingounis, A. V., and Jahr, C. E. (2002) Comparison of coupled and uncoupled currents during glutamate uptake by GLT-1 transporters, *J. Neurosci. 22*, 10153−10162.
28. Otis, T. S., and Jahr, C. E. (1998) Anion currents and predicted glutamate flux through a neuronal glutamate transporter, *J. Neurosci. 18*, 7099−7110.
29. Wadiche, J. I., and Kavanaugh, M. P. (1998) Macroscopic and microscopic properties of a cloned glutamate transporter/chloride channel, *J. Neurosci. 18*, 7650−7661.
30. Shimamoto, K., Lebrun, B., Yasuda-Kamatani, Y., Sakaitani, M., Shigeri, Y., Yumoto, N., and Nakajima, T. (1998) DL-threo-β-benzyloxyaspartate, a potent blocker of excitatory amino acid transporters, *Mol. Pharm. 53*, 195−201.
31. Campiani, G., De Angelis, M., Armaroli, S., Fattorusso, C., Catalanotti, B., Ramunno, A., Nacci, V., Novellino, E., Grewer, C., Ionescu, D., Rauen, T., Griffiths, R., Sinclair, C., Fumagalli, E., and Mennini, T. (2001) A rational approach to the design of selective substrates and potent nontransportable inhibitors of the excitatory amino acid transporter EAAC1 (EAAT3). New glutamate and aspartate analogues as potential neuroprotective agents, *J. Med. Chem. 44*, 2507−2510.
32. Grewer, C., and Grabsch, E. (2004) New inhibitors for the neutral amino acid transporter ASCT2 reveal its Na^+-dependent anion leak, *J. Physiol. 557*, 747−759.
33. Tao, Z., and Grewer, C. (2005) The conserved histidine 295 does not contribute to proton cotransport by the glutamate transporter EAAC1, *Biochemistry 44*, 3466−3476.
34. Pines, G., Zhang, Y., and Kanner, B. I. (1995) Glutamate 404 is involved in the substrate discrimination of GLT-1, a ($Na^+ + K^+$)-coupled glutamate transporter from rat brain, *J. Biol. Chem. 270*, 17093−17097.
35. Yernool, D., Boudker, O., Folta-Stogniew, E., and Gouaux, E. (2003) Trimeric subunit stoichiometry of the glutamate transporters from *Bacillus caldotenax* and *Bacillus stearothermophilus*, *Biochemistry 42*, 12981−12988.
36. Schwartz, E. A., and Tachibana, M. (1990) Electrophysiology of glutamate and sodium co-transport in a glial cell of the salamander retina, *J. Physiol. 426*, 43−80.
37. Conradt, M., and Stoffel, W. (1995) Functional analysis of the high affinity, Na^+-dependent glutamate transporter GLAST-1 by site-directed mutagenesis, *J. Biol. Chem. 270*, 25207−25212.
38. Kanai, Y., Nussberger, S., Romero, M. F., Boron, W. F., Hebert, S. C., and Hediger, M. A. (1995) Electrogenic properties of the epithelial and neuronal high affinity glutamate transporter, *J. Biol. Chem. 270*, 16561−16568.
39. Billups, B., and Attwell, D. (1996) Modulation of non-vesicular glutamate release by pH, *Nature 379*, 171−174.
40. Grewer, C., and Rauen, T. (2005) Electrogenic glutamate transport in the CNS: Molecular mechanism, pre-steady-state kinetics, and their impact on synaptic signaling, *J. Membr. Biol. 203*, 1−20.
41. Koch, H. P., and Larsson, H. P. (2005) Small-scale molecular motions accomplish glutamate uptake in human glutamate transporters, *J. Neurosci. 25*, 1730−1736.

BI050987N